ChemComm
www.rsc.org/chemcomm

Tuning of particle morphology and pore properties in mesoporous silicas with multiple organic functional groups†

Seong Huh,[ab] Jerzy W. Wiench,[b] Brian G. Trewyn,[a] Seahn Song‡,[a] Marek Pruski[b] and Victor S.-Y. Lin*[ab]

[a] Department of Chemistry, Iowa State University, Ames, Iowa 50011-3111. E-mail: vsylin@iastate.edu;
   Tel: +1 515-294-3135
[b] Ames Laboratory, Iowa State University, Ames, Iowa 50011-3020

A synthetic method has been developed that can control both multifunctionalization and morphology of the mesoporous organic–inorganic hybrid materials by introducing different molar ratios of organoalkoxysilane precursors to a base-catalyzed co-condensation of silicate.

Recent advances in synthesizing organically functionalized mesoporous silicas[1] have highlighted the potential of utilizing these materials as selective catalysts,[1b,2] adsorbents,[3] and sensors.[4] Further progress in such applications will rely on the ability to tune the extent of functionalization with multiple organic moieties and to control the particle morphology in order to direct the mass-transport properties of the resulting *organic–inorganic* hybrid materials. Morphology control of inorganic mesoporous silicas has been studied intensively ever since the first report of MCMs family a decade ago. The desired particle shapes were prepared *via* pH control,[5] utilization of base catalysts,[6] and by the use of co-solvents,[7] *e.g.* in a modified Stoeber process.[7c,d] We describe herein a new approach, in which various organoalkoxysilane precursors introduced during the co-condensation reactions, rather than the co-solvents, are used for morphology control. An added advantage of this method is that it results in simultaneous anchoring of multiple functional groups to the mesopores (multifunctionalization). The roles and quantities of these moieties may be tailored independently and/or cooperatively for various applications, such as gatekeeping. To the best of our knowledge, the synthetic pathway that controls both *multifunctionalization* and *morphology* of such hybrid materials has not been reported before.

The FE-SEM images of two mesoporous silicas functionalized through the introduction of 3-[2-(2-aminoethylamino)ethylamino]propyl (AEP) and 3-cyanopropyl (CP) as organoalkoxysilane precursors, are shown in Fig. 1a and b, respectively.†
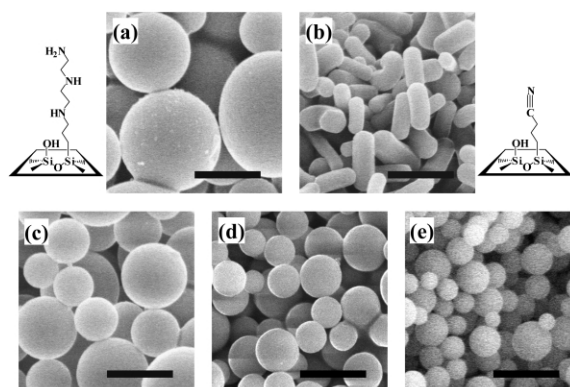
In contrast to the pure MCM-41 synthesized under the same conditions, which exhibits irregular spherical shape,† monofunctionalization with AEP or CP resulted in different particle shapes and sizes, *i.e.*, spheres with an average diameter = 3 μm and rods with an average size of 1 × 0.2 μm. These materials were prepared by sodium hydroxide-catalyzed condensation reactions of tetraethoxysilane (TEOS) with AEP-trimethoxysilane (AEPTMS) or CP-triethoxysilane (CPTES), in the presence of a low concentration of cetyltrimethylammonium bromide (CTAB) surfactant, under stirring (550 rpm) at 80 °C for 2 h. The reaction mixture molar ratio was 1.00 CTAB : 8.16 TEOS : 1.05 total organoalkoxysilanes : 2.55 NaOH : 4857 H_2O. Surfactant-free materials were obtained with an acid extraction.† The observed difference in particle morphology prompted us to synthesize a series of bifunctional materials in which the molar ratio between AEPTMS and CPTES was varied from 100% AEPTMS to 100% CPTES, with the total amount of AEPTMS + CPTES relative to TEOS fixed at 12.8 mol%. Herein, we will refer to the monofunctionalized microparticle (MP) as AEP-MP (CP-MP) and to the bifunctionalized materials as AEP/CP-MP.

As depicted in Fig. 1c, d, and e, the FE-SEM micrographs of the AEP/CP-MP materials synthesized with different molar ratios of AEPTMS/CPTES showed only spherical particles. In contrast to the micron-sized AEP-MP, the average diameters of the AEP/CP-MP spheres decreased as the relative ratio of AEPTMS/CPTES changed from 5/5 to 1/9. It is interesting to note that even in the 1/9 case (1.28 mol % of AEPTMS and 11.52 mol % of CPTES, Fig. 1e), no rod-like particles were observed, which is in stark contrast with CP-MP sample (12.8 mol % of CPTES, Fig. 1b). Evidently, the presence of AEPTMS precursor in the co-condensation reaction played a crucial role in governing the particle shape.

The influence of organoalkoxysilanes on the pore properties and structure was studied using the powder XRD diffraction patterns. As shown in Fig. 2a and in the ESI,† the observed patterns exhibited a strong d_{100} peak and a broad peak derived from the combination of d_{110} and d_{200} diffractions, most likely due to a disordered wormhole-like porous structure. This observed diffraction pattern is very similar to that of the AEP-MP material. Also, the TEM micrographs† revealed the disordered, wormhole pore structure in both AEP-MP and AEP/

Fig. 1 FE-SEM images of (a) AEP-MP, (b) CP-MP, (c) 5/5 AEP/CP-MP, (d) 3/7 AEP/CP-MP, (e) 1/9 AEP/CP-MP. Scale bar = 1 μm.

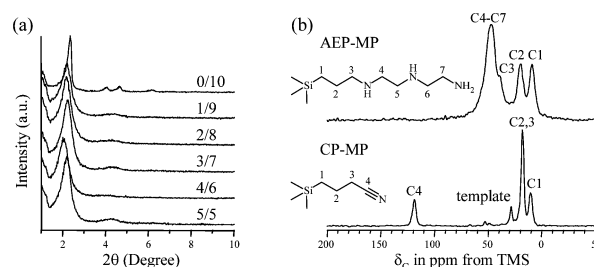**Fig. 2** (a) Powder XRD diffraction patterns of materials synthesized with different molar ratios of AEPTMS/CPTES. (b) ^{13}C CPMAS NMR spectra of AEP-MP and CP-MP.

CP-MP. Interestingly, the XRD (Fig. 2a) and TEM measurements of the CP-MP rods showed a typical MCM-41 type of hexagonal symmetry of the mesopores packed in a parallel fashion along the long axis of the rod-shaped particles. These observations provided further evidence that the sample morphology is very sensitive to the presence of AEPTMS during co-condensation.

^{13}C solid-state NMR was used to (i) obtain spectroscopic evidence for the presence of the organic moieties in the mesopores, (ii) confirm their chemical structure, and (iii) measure their relative concentration. The spectra were obtained at 9.4 T on a Varian/Chemagnetics Infinity spectrometer, using ^{1}H–^{13}C cross polarization with magic angle spinning (CPMAS).[8] The spectra, shown in Fig. 2b, demonstrated that the mesopores were indeed functionalized as intended.

Measurements of the "build-up" of carbon magnetization during cross-polarization revealed details about the molecular motions of both functional groups and allowed to measure their relative concentration in all samples.† In AEP-MP, all CH_2 carbons were polarized with a time constant τ_{CH} on the order of 60 μs, which is typical for such functional groups when they are sufficiently rigid (in this case, do not undergo motions on a kHz scale). A similar time constant has been found for the C1 carbon in CP-MP. However, the evolution of resonance at 19 ppm assigned to the C2 and C3 groups in this sample involved two time constants of approximately 100 and 700 μs. This result showed that the C2–H_2 and C3–H_2 groups in CP-MP experienced increasing mobility, which weakened the ^{1}H–^{13}C dipolar coupling and inhibited the cross polarization process. The τ_{CH} value of 5 ms observed for carbon C4 was consistent with the nitrile end of CP-MP being the most mobile.

Our measurements also showed that in the AEP/CP-MP samples the cross polarization dynamics was the same, within the experimental error, as for the corresponding carbon species in AEP-MP and CP-MP. This allowed us to use the physical mixture of AEP-MP with CP-MP in a known molar ratio as the intensity standard for quantitative analysis of the spectra of bifunctionalized samples, which are shown in Fig. 3. Two unique resonances, at around 48 ppm in AEP (carbons C4–C7) and at 120 ppm in CP (carbon C4), offered best indicators of both functionalities. The exact procedure used for quantitative measurements is described in the ESI.†

In order to investigate the *chemical accessibility* of the organic functional groups, we examined the Cu^{2+} adsorption capacity of representative samples.[9] Because of the chelate effect of the diethylene triamine moiety of the AEP group, we anticipated significantly higher Cu^{2+} adsorption capacities for the materials with higher amount of AEP. Indeed, our results indicated that the AEP-MP and CP-MP materials showed
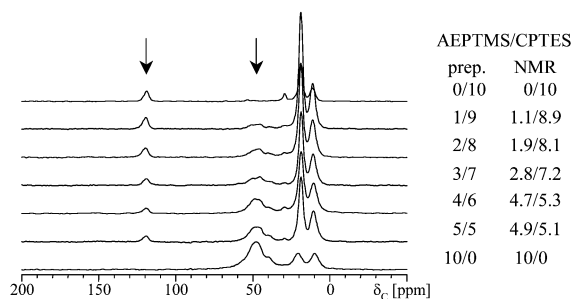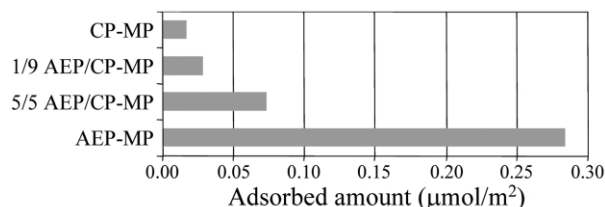
Fig. 4 Diagram of Cu(II) adsorption capacity for selected samples.

adsorptivities of 0.284 and 0.017 μmol m^{-2}, respectively (Fig. 4). The corresponding values for 5/5 and 1/9 AEP/CP-MP silicas were 0.073 and 0.028 μmol m^{-2}. We note, however, that the Cu^{2+} adsorption capacity increased by a factor of only 2.6 between the 1/9 to 5/5 AEP/CP-MP samples, whereas solid state NMR showed an 8-fold increase of the relative AEP/CP ratio. Given that the total loading of both organic groups was fixed at 12.8 mol %, these results indicated that the chemical accessibility did not increase linearly with the amount of AEP groups in bifunctional silicas. The CP functionality, which is hydrophobic in nature, might have played an active role in decreasing the adsorption capacity per AEP group.

Notes and references

1 (a) M. H. Lim, C. F. Blanford and A. Stein, *J. Am. Chem. Soc.*, 1997, **119**, 4090; (b) A. Stein, B. J. Melde and R. C. Schroden, *Adv. Mater.*, 2000, **12**, 1403; (c) C. E. Fowler, S. Mann and B. Lebeau, *Chem. Commun.*, 1998, 1825; (d) S. Inagaki, S. Guan, T. Ohsuna and O. Terasaki, *Nature*, 2002, **416**, 304; (e) H. Fan, Y. Lu, A. Stump, S. T. Reed, T. Baer, R. Schunk, V. Perez-Luna, G. P. Lopez and C. J. Brinker, *Nature*, 2000, **405**, 56.

2 (a) V. S.-Y. Lin, D. R. Radu, M.-K. Han, W. Deng, S. Kuroki, B. H. Shanks and M. Pruski, *J. Am. Chem. Soc.*, 2002, **124**, 9040; (b) J. Y. Ying, C. P. Mehnert and M. S. Wong, *Angew. Chem., Int. Ed.*, 1999, **38**, 56; (c) A. Sayari, *Chem. Mater.*, 1996, **8**, 1840; (d) K. Moller and T. Bein, *Chem. Mater.*, 1998, **10**, 2950; (e) X. He and D. Antonelli, *Angew. Chem., Int. Ed.*, 2002, **41**, 214; (f) K. Kageyama, J.-I. Tamazawa and T. Aida, *Science*, 1999, **285**, 2113; (g) M. E. Davis, *Nature*, 2002, **417**, 813.

3 (a) S. Dai, M. C. Burleigh, Y. Shin, C. C. Morrow, C. E. Barnes and Z. Xue, *Angew. Chem., Int. Ed.*, 1999, **38**, 1235; (b) J. Brown, L. Mercier and T. J. Pinnavaia, *Chem. Commun.*, 1999, 69; (c) X. Feng, G. E. Fryxell, L. Q. Wang, A. Y. Kim, J. Liu and K. M. Kemner, *Science*, 1997, **276**, 923.

4 (a) V. S.-Y. Lin, C.-Y. Lai, J. Huang, S.-A. Song and S. Xu, *J. Am. Chem. Soc.*, 2001, **123**, 11510; (b) G. Wirnsberger, B. J. Scott and G. D. Stucky, *Chem. Commun.*, 2001, 119; (c) A. B. Descalzo, D. Jimenez, M. D. Marcos, R. Martinez-Manez, J. Soto, J. El Haskouri, C. Guillem, D. Beltran, P. Amoros and M. V. Borrachero, *Adv. Mater.*, 2002, **14**, 966.

5 (a) H.-P. Lin and C.-Y. Mou, *Acc. Chem. Res.*, 2002, **35**, 927; (b) Q. Huo, D. Zhao, J. Feng, K. Weston, S. K. Buratto, G. D. Stucky, S. Schacht and F. Schuth, *Adv. Mater.*, 1997, **9**, 974; (c) G. A. Ozin, *Chem. Commun.*, 2000, 419.

6 Q. Cai, Z.-S. Luo, W.-Q. Pang, Y.-W. Fan and X.-H. Chen and F.-Z. Cui, *Chem. Mater.*, 2001, **13**, 258.

7 (a) M. T. Anderson, J. E. Martin, J. G. Odinek and P. P. Newcomer, *Chem. Mater.*, 1998, **10**, 1490; (b) D. Zhao, J. Sun, Q. Li and G. D. Stucky, *Chem. Mater.*, 2000, **12**, 275; (c) M. Etienne, B. Lebeau and A. Walcarius, *New J. Chem.*, 2002, **26**, 384; (d) K. Schumacher, C. Du Fresne von Hohenesche, K. K. Unger, R. Ulrich, A. Du Chesne, U. Wiesner and H. W. Spiess, *Adv. Mater.*, 1999, **11**, 1194 and the references therein.

8 A. Pines, M. G. Gibby and J. S. Waugh, *J. Chem. Phys.*, 1973, **59**, 569.

9 M. C. Burleigh, M. A. Markowitz, M. S. Spector and B. P. Gaber, *Chem. Mater.*, 2001, **13**, 4760.

Fig. 3 ^{13}C CPMAS spectra of AEP/CP-MP's. Arrows show the resonances that are unique for each species and thus were used for quantitative analysis. The numbers represent the molar ratio between two components used for preparation and obtained from analysis of NMR spectra.